Princeton Plasma Physics Laboratory

PPPL-4044rev
PPPL-4044rev

Progress towards Steady State on NSTX

D.A. Gates, C. Kessel, J. Menard, G. Taylor, J.R. Wilson,
and 94 additional co-authors

January 2005
Revised March 2005

Prepared for the U.S. Department of Energy under Contract DE-AC02-76CH03073.

PPPL Report Availability

This report is posted on the U.S. Department of Energy's Princeton Plasma Physics Laboratory Publications and Reports web site in Fiscal Year 2005. The home page for PPPL Reports and Publications is: http://www.pppl.gov/pub_report/

Office of Scientific and Technical Information (OSTI):

Available electronically at: http://www.osti.gov/bridge.

Available for a processing fee to U.S. Department of Energy and its contractors, in paper from:

U.S. Department of Energy
Office of Scientific and Technical Information
P.O. Box 62
Oak Ridge, TN 37831-0062

Telephone: (865) 576-8401

Fax: (865) 576-5728

E-mail: reports@adonis.osti.gov

National Technical Information Service (NTIS):

This report is available for sale to the general public from:

U.S. Department of Commerce
National Technical Information Service
5285 Port Royal Road
Springfield, VA 22161

Telephone: (800) 553-6847

Fax: (703) 605-6900

Email: orders@ntis.fedworld.gov

Online ordering: http://www.ntis.gov/ordering.htm

Progress towards steady state on NSTX

D. A. Gates[1], C. Kessel[1], J. Menard[1], G. Taylor[1], J.R. Wilson[1], M.G. Bell[1], R.E. Bell[1], S. Bernabei[1], J. Bialek[2], T. Biewer[1], W. Blanchard[1], J. Boedo[3], C. Bush[4], M.D. Carter[4], W. Choe[5], N. Crocker[6], D.S. Darrow[1], W. Davis[1], L. Delgado-Aparicio[7], S. Diem[1], J. Ferron[8], A. Field[9], J. Foley[1], E.D. Fredrickson[1], T. Gibney[1], R. Harvey[10] R.E. Hatcher[1], W. Heidbrink[11], K. Hill[1], J.C. Hosea[1], T.R. Jarboe[12], D.W. Johnson[1], R. Kaita[1],S. Kaye[1], S. Kubota[6], H.W. Kugel[1], J. Lawson[1], B.P. LeBlanc[1], K.C. Lee[13], F. Levinton[14], R. Maingi[4], J. Manickam[1], R. Maqueda[14], R. Marsala[1], D. Mastrovito[1], T.K. Mau[3], S.S. Medley[1], H. Meyer[9], D.R. Mikkelsen[1], D. Mueller[1], T. Munsat[15], B.A. Nelson[12], C. Neumeyer[1], N. Nishino[16], M. Ono[1], H. Park[1], W. Park[1], S. Paul[1], T. Peebles[6], M. Peng[4], C. Phillips[1], A. Pigarov[3], R. Pinsker[8], A. Ram[17], S. Ramakrishnan[1], R. Raman[12], D. Rasmussen[4], M. Redi[1], M. Rensink[18], G. Rewoldt[1], J. Robinson[1], P. Roney[1], L. Roquemore[1], E. Ruskov[11], P. Ryan[4], S.A. Sabbagh[2], H. Schneider[1], C.H. Skinner[1], D.R. Smith[1], A. Sontag[2], V. Soukhanovskii[18], T. Stevenson[1], D. Stotler[1], B. Stratton[1], D. Stutman[7], D. Swain[4], E. Synakowski[1], Y. Takase[19], K. Tritz[7], A. von Halle[1], M. Wade[4], R. White[1], J. Wilgen[4], M. Williams[1], W. Zhu[2], S.J. Zweben[1], R. Akers[9], P. Beiersdorfer[18], R. Betti[20], T. Bigelow[4]

[1] *Princeton Plasma Physics Laboratory, Princeton University, Princeton, NJ 08543, USA*
[2] *Dept. of Applied Physics, Columbia Univ., NYC, NY, USA*
[3] *University of California, San Diego, CA, USA*
[4] *Oak Ridge National Laboratory, Oak Ridge, TN, USA*
[5] *Korea Advanced Institute of Science and Technology, Taejon, Republic of Korea*
[6] *University of California, Los Angeles, CA, USA*
[7] *Johns Hopkins University, Baltimore, MD, USA*
[8] *General Atomics, San Diego, CA, USA*
[9] *Euratom-UKAEA Fusion Associates, Abingdon, Oxfordshire, UK*
[10] *CompX, Del Mar, CA, USA*
[11] *University of California, Irvine, CA, USA*
[12] *University of Washington, Seattle, WA, USA*
[13] *University of California, Davis, CA, USA*
[14] *Nova Photonics, Princeton, NJ, USA*
[15] *University of Colorado, Boulder, CO, USA*
[16] *Hiroshima University, Hiroshima, Japan*
[17] *Massachusetts Institute of Technology, Cambridge, MA, USA*
[18] *Lawrence Livermore National Laboratory, Livermore, CA, USA*
[19] *Tokyo University, Tokyo, Japan*
[20] *University of Rochester, Rochester, NY, USA*

Abstract

In order to reduce recirculating power fraction to acceptable levels, the spherical torus concept relies on the simultaneous achievement of high toroidal β and high bootstrap fraction in steady state. In the last year, as a result of plasma control system improvements, the achievable plasma elongation on NSTX has been raised from $\kappa \sim 2.1$ to $\kappa \sim 2.6$ - approximately a 25% increase. This increase in elongation has lead to a substantial increase in the toroidal β for long pulse discharges. The increase in β is associated with an increase in plasma current at nearly fixed poloidal β, which enables higher β_t with nearly constant bootstrap fraction. As a result, for the first time in a spherical torus, a discharge with a plasma current of 1MA has been sustained for 1 second. Data is presented from NSTX correlating the increase in performance with increased plasma shaping capability. In addition to improved shaping, H-modes induced during the current ramp phase of the plasma discharge have been used to reduce flux consumption and to delay the onset of MHD instabilities. A modeled integrated scenario, which has 100% non-inductive current drive with very high toroidal β, will also be discussed. The NSTX poloidal field coils are currently being modified to produce the plasma shape which is re-

quired for this scenario, which requires high triangularity ($\delta \sim 0.8$) at elevated elongation ($\kappa \sim 2.5$). The other main requirement for steady state on NSTX is the ability to drive a fraction of the total plasma current with RF waves. The results of High Harmonic Fast Wave heating and current drive studies as well as electron Bernstein Wave emission studies will be presented.

1. Introduction

The Spherical Torus [1] concept is an extension of the same thought process that leads to the steady-state advanced tokamak concept. Using the bootstrap current and external non-inductive current drive to sustain a tokamak in steady state is an immediate precursor to the concept of changing the geometry of the torus to optimize bootstrap current and minimize the need for an ohmic transformer. The Spherical Torus takes the extreme step of eliminating the transformer and maximizing toroidal field utilization by reducing the physical size of the toroidal field coil to engineering limits. This extreme geometry leads to challenges. In particular, as the aspect ratio is reduced, the ability to shield the center column of the toroidal coil is reduced. In the low aspect ratio limit, it becomes impossible to use known superconducting materials to build the toroidal field coil for a reactor due to the nuclear heating. This lack of shielding then requires low aspect ratio devices to employ conventional conductors, which in turn forces the device to operate at very high toroidal β so as to minimize the recirculating power fraction. Fortunately nature cooperates since the achievable β is increased at low aspect ratio. In addition to the higher β limits, the achievable elongation is also higher at low aspect ratio. This is important since the bootstrap fraction at fixed β_N and $q^\star$ scales like $\sim \sqrt{1+\kappa^2}$ [where $\beta_N \equiv \beta_t * aB_t/I_p$, with $\beta_t \equiv 2\mu_0 P/B_t^2$, and $q^\star \equiv \pi a^2\sqrt{1+\kappa^2}B_t/(\mu_0 R I_p)$].

The National Spherical Torus Experiment [2] is a low aspect ratio torus ($A = R/a \sim 1.3$, where A is the aspect ratio, R is the major radius of the torus and a is the minor radius of the torus). NSTX has previously achieved $\beta_t \sim 35\%$ and non-inductive current fractions of $\sim 60\%$ [3], albeit not simultaneously. Recently, the operating regime of the device has been expanded to help explore the high κ operating space that has been identified as most attractive for the ST concept. The consequence of this expanded operating regime was a substantial improvement in the achievable β_t in long pulse discharges, as expected by MHD stability theory and neoclassical theory. The details of the observed improvement will be discussed in Section 2. In addition to the improved shaping capability, H-modes were triggered during the current ramp. The improvements to the flux consumption due to this early transition are described in Section 3. Integrated scenario modeling indicates that scenarios exist which have 100% non-inductive current drive at $\beta_t \sim 40\%$. Results from these calculations as well as machine modifications in support of developing this scenario will be presented in Section 4. NSTX also is investigating external non-inductive current drive options. In particular, NSTX has successfully driven current using the High Harmonic Fast Waves (HHFW). Results from both heating and current drive experiments will be discussed in Section 5. Future plans include using Electron Bernstein Waves (EBW) for external current drive and electron heating. Results from EBW emission experiments will also be discussed in Section 5.

2. Widened operating regime

The improvement in operating regime for NSTX was achieved primarily by improving plasma control capabilities. In particular, the digital control system on NSTX was improved to reduce the control latency. The control latency (defined as the propagation time of a perturbation through the control system) is an important parameter for determining the maximum gain in a control loop. The average latency in the NSTX control system was reduced by a factor of 4 to $\sim 0.75ms$, primarily through hardware upgrades. This led to an increase in the sustainable plasma elongation from a previous high of $\kappa \sim 2.1$ to a new high $\kappa \sim 2.6$. Shown in Figure 1 is a plot of the achieved plasma elongation as determined by the EFIT equilibrium reconstruction code [4, 5] versus the normalized internal inductance l_i, also determined by EFIT. As can be seen in Figure 1 the increase in κ is $\sim 20\%$ at fixed l_i. In addition to the improvements in the control latency, an analog measurement of the vertical voltage difference was added to improve the fidelity of the derivative term in the vertical position control loop.

The improvement in κ has led to a corresponding increase in the β_t attainable for long pulse discharges. Time histories of the plasma current and β_t for a best case example discharge is shown in Figure 2. As can be seen from the Figure, the plasma current is increased by 25%, the toroidal field current is decreased by $\sim$ 10% and the pulse length is nominally increased. Accordingly the peak β_t is increased by $\sim$ 50%. Additionally, the plasma stored energy does not drop until the end of the discharge which further increases the pulse averaged β_t. The change in plasma cross-section for the plasma discharges shown in Figure 2 are shown in Figure 3. The green boundary in the Figure is the lower κ, lower β_t discharge.

To help quantify the connection between the increase in plasma elongation and the observed improvement in performance, we plot the pulse averaged β_t versus the pulse length over which the averaging was performed for the entire NSTX database 4. In the first frame of the plot the data is color sorted by year, whereas in the second frame, the color sorting is by elongation. As is apparent in the plot, the improvement in pulse average β_t is clearly correlated with the increase in plasma elongation that came along with the control system improvements for 2004.

In order to understand the role of bootstrap current in increasing the pulse averaged β, a new parameter is defined which is particularly relevant to the spherical torus concept. The parameter which will be referred to as the sustained β fraction is defined as $\beta_{sus} \equiv 0.5\sqrt{\varepsilon}\beta_p \times \beta_t \sim f_{bs} \times \beta_t$, where $\varepsilon \equiv a/R$, $\beta_p \equiv 2\mu_0\langle P\rangle/\bar{B}_p^2$ (where $\bar{B}_p$ is the poloidal magnetic field averaged over the plasma minor circumference), and $f_{bs} \equiv I_{bs}/I_p$ is the bootstrap current fraction. There is an intrinsic trade off between plasma current and bootstrap fraction and hence, since the ideal β limit is proportional to plasma current, there is also a trade off between β_t and the bootstrap fraction. This β_{sus} parameter balances this trade-off and therefore more directly defines high performance in plasmas that depend on both bootstrap fraction and high β_t for viability as fusion devices. The advanced tokamak concept, which also relies upon the bootstrap current for sustainment and high β_t, could also make use of this parameter in defining progress.

Figure 5 shows the pulse averaged value of the sustained β for the NSTX database plotted versus the quantity $1 + \kappa^2$ (one can simply show that $f_{bs} \times \beta_t \sim \beta_N^2(1 + \kappa^2)$ assuming a plasma of elliptical cross-section). If the upper bound of the sustained β parameter is determined by the ideal MHD β-limit, then to the degree that the elliptical approximation is adequate, plasma elongation is the only controlling variable remaining. In principle, it should also be possible to optimize the sustained β by raising the limiting β_N through various other control techniques, but that is not the focus of this paper. It is interesting to note that the data seems to improve more rapidly with increasing elongation than is predicted by the simple model. The cause for this is apparent in Figure 2. There is a partial β collapse in the lower current, lower β_t plasma before the end of the plasma current flattop, whereas the high β phase persists until the end of the higher elongation plasma. A possible explanation for the delayed onset of instability in recent discharges is the lower plasma inductance which was in turn due to the inducement of H-mode during the current ramp of the higher elongation discharge.

3. Early H-mode

The technique of inducing H-mode during the current ramp by use of a small pause or "flat-spot" in the current ramp, which has been used on many different devices (see, e.g., Reference [6]), has recently been applied on NSTX [7]. Shown in Figure 6 is a comparison between two plasma discharges, one with an induced early H-mode transition and one without. As is apparent in the Figure, the flux consumption is noticeably reduced during the current ramp phase of the discharge with the early H-mode transition. (The flux consumption is proportional to the change in flux in the ohmic heating coil). The reason for the reduced flux consumption is three-fold: The electron temperature profile broadens thereby reducing the plasma resistance, the pressure profile broadens increasing the bootstrap current, and the broader pressure profile actually permits the achievement of higher β due to increased MHD stability with broad pressure profiles.

The broader profiles delay the onset of deleterious MHD, which still is the primary cause of plasma termination. The limiting MHD is believed to be due to the relaxation of the residual inductively driven current into the core of the discharge. Work is ongoing to analyze the MHD stability of these discharges using the recently commissioned Motional Stark Effect polarimetry diagnostic to verify understanding of the behavior of these long pulse discharges.

4. Integrated scenario modeling

Recent modeling efforts using the modeling codes TSC [8] and TRANSP [9] have identified an attractive scenario that is fully non-inductively sustained with $\beta_t \sim 40\%$ [10]. This scenario incorporated calculations of EBW and beam driven current as well as bootstrap current. The modeled plasma is calculated to be stable to $n = 1$ ideal MHD modes in the presence of an ideal conducting wall. The scenario identified requires strong plasma shaping with the simultaneous achievement of high elongation ($\kappa \sim 2.5$) and high triangularity ($\delta \sim 0.8$). Equilibrium calculations indicated that this was not possible with the original NSTX poloidal field coil set. As a result, the PF1A coils (indicated in Figure 7) have been modified, in order to produce the plasma identified through modeling. Also shown in Figure 7 is a comparison between a typical double-null, high-elongation shot from 2004 and a calculated equilibrium using the same plasma profiles but the modified PF1A coil set. The modified poloidal field coils will be used to investigate the long pulse behavior of these highly shaped plasma discharges in the coming year. The modeled scenario requires a functional non-inductive current drive mechanism (e.g. those described in the next section) to provide $\sim 10\%$ of the plasma current.

5. HHFW and EBW heating and current drive

High Harmonic Fast Wave (HHFW) heating has been proposed as an attractive means for heating and driving current in an ST. The NSTX HHFW heating system consists of a twelve strap antenna connected to 6 independent RF sources [11]. The total power available from the system is 6MW. Experiments have been performed which demonstrate that significant heating power can be deposited on the electrons and that current can be driven with directed waves.The surface voltage from two plasma discharges, one with co-phasing and one with counter, are shown in Figure 8. Because the heating efficiency is observed to vary substantially between the different phasings, the total power was adjusted so that the electron temperatures match. Four different electron temperature profiles, two from each shot, are overlaid in Figure 9 indicating the quality of the temperature match. The difference in loop voltage is calcualted to a correspond to a total difference in HHFW driven current of 180kA between the two cases. The plasma current in these discharges is 500kA.

High Harmonic Fast Waves (HHFW) have also been observed to damp on both edge thermal ions and fast particles injected by neutral beam heating. This ion damping behavior is an important feature of High Harmonic

Fast Wave heating that must be more fully understood so as to avoid undesired diversion of current drive power into bulk ion heating, thereby effectively reducing the current drive efficiency. Work is ongoing to develop better understanding of the physics that controls HHFW ion damping, but initial indications are that the fast ion heating is due to direct wave damping [12], whereas the edge bulk heating is due to parametric decay into an ion Bernstein mode and an ion quasi-mode [13].

Theoretical calculations have indicated that Electron Bernstein Waves (EBW) may be an efficient method for heating electrons and driving current in NSTX, particularly at high β [14]. Since NSTX operates well into the overdense regime (where $\omega_{pe} >> \omega_{ce}$, where ω_{pe} is the electron plasma frequency and ω_{ce} the electron cyclotron frequency) conventional electron cyclotron heating is not viable. However, EBWs can propagate in such plasmas and are strongly absorbed at harmonics of the cyclotron frequency. Detailed numerical modeling has also indicated that these waves can be used to efficiently drive off-axis current, in keeping with the requirement indicated by integrated scenario modeling .

In order for the heating scheme to work, a conversion scheme is needed to couple power from the electromagnetic wave launched by a microwave antenna to the electrostatic wave that is capable of propagating inside the plasma boundary. A scheme has been proposed which couples the O-mode electromagnetic wave to the Bernstein wave. Recent measurements of EBW emission support the viability of this coupling mechanism [15]. Radiometer measurements of the emitted EBW have confirmed that there is indeed efficient emission of waves in the EBW range of frequencies at the viewing angle where the coupling condition is satisfied.

6. Summary

NSTX is developing and incorporating numerous tools to simultaneously achieve high bootstrap fraction and high toroidal β. Improved control capability has already broadened the long pulse operating regime substantially. Induced early H-mode transitions have reduced plasma internal inductance which in turn has delayed the onset of pulse limiting MHD. Progress has been made on both HHFW heating and current drive and EBW emission studies. Integrated scenario modeling has identified a steady state scenario that is stable at $\beta_t \sim 40\%$. The NSTX poloidal field coil set has been modified to enable the achievement of this scenario. The advances to date on NSTX represent significant progress towards demonstrating the viability of the ST concept for magnetic fusion.

This work was supported by the U.S. Department of Energy Grant under contract number DE-AC02-76CH03073.

References

[1] Y-K. M. Peng and D. J. Strickler, Nucl. Fusion **26**, 769 (1986)

[2] M. Ono, S. M. Kaye, Y. -K. M. Peng, *et al.*, Nucl. Fusion **40**, 557 (2000)

[3] D. A. Gates and the NSTX national research team, Phys. Plasmas, **10**, 1659 (2003)

[4] S. A. Sabbagh, R. E. Bell, M. G. Bell, et al., Nucl. Fusion **41**, 1601 (2001)

[5] L. L. Lao, H. St. John, R. D. Stambaugh, et al., Nucl. Fusion **25**, 1421 (1985)

[6] M.R.Wade, M. Murakami, T.C. Luce, J.R. Ferron, C.C. Petty, et al., Nucl. Fusion **43**, 634 (2003)

[7] J.E. Menard, R.E. Bell, E.D. Fredrickson, D.A. Gates, S.M. Kaye, et al., presented at the 20th Fusion Energy Conference, Vilamoura, Portugal (2004), submitted to Nucl. Fusion (2005)

[8] S. Jardin, N. Pomphrey, and J. Delucia, J. Comput. Phys. **66**, 481 (1986)

[9] R.J. Hawryluk, in Physics of Plasmas Close to Thermonuclear Conditions **1** 19 (CEC, Brussels, 1980)

[10] C. E. Kessel, E. J. Synakowski, M. E. Bell, D. A. Gates, R. W. Harvey, et al., presented at the 20th Fusion Energy Conference, Vilamoura, Portugal (2004), submitted to Nucl. Fusion (2005)

[11] J. R. Wilson, R. E. Bell, S. Bernabei, et al., Phys. Plasmas **10**, Part 2 1733 (2003)

[12] A.L. Rosenberg, J.E. Menard, J.R. Wilson, S. Medley, C.K. Phillips, et al., Phys. Plasmas **11** 2441 (2004)

[13] T. Biewer, et al., to be published in Phys. Plasmas (2005)

[14] G. Taylor, P.C. Efthimion, C.E. Kessel, R.W. Harvey, A.P. Smirnov, et al., Phys. Plasmas **11**, 4733 (2004)

[15] G. Taylor, to be published in Phys. Plasmas (2005)

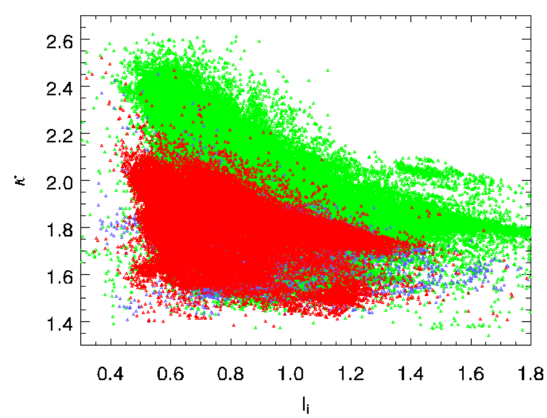

Figure 1: Plot of the vertical stability space of the entire NSTX database, plotting plasma elongation (κ) vs. normalized internal inductance (l_i). Each point represents a single timeslice of an NSTX plasma discharge. Values are calculated using the EFIT ideal MHD equilibrium reconstruction code.

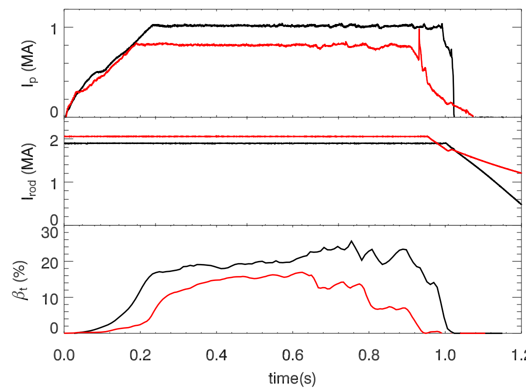

Figure 2: Comparison of the "best" shots from 2004 (after control improvements, black) and from 2002 (before control improvements, red). Shown in each panel are a) plasma current (MA), b) total current in the toroidal field central rod (MA), and c) β_t (from EFIT) all vs. time. Plasma current is increased by 25%, TF current is reduced by 10%, and β_t is correspondingly increased by a factor of two (pulse averaged).

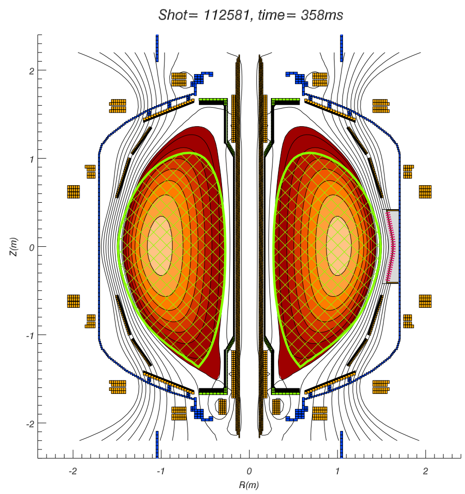

Figure 3: Overlay of the boundaries of the plasma discharges show in Figure 2. Plasma elongation is $\kappa \sim 2.1$ for shot 109063 (green) and $\kappa \sim 2.5$ for shot 112581 (red)

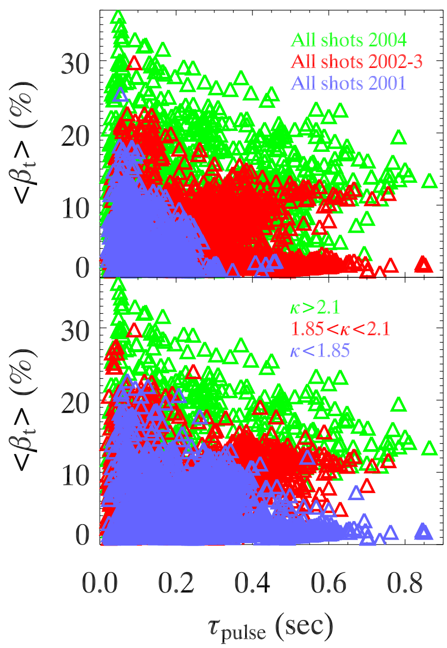

Figure 4: Plot of the pulse average β_t versus the pulse length over which $beta_t$ was averaged. The pulse length is determined from the plasma current flattop. Each point represents one plasma in the NSTX database, with the entire database plotted. In the first frame the shots are sorted by year as indicated. In the second frame, the shots are sorted by elongation, indicating the correlation between the increase in achievable plasma elongation and the increase in β_t.

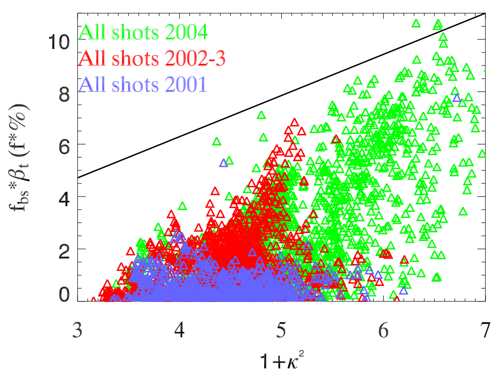

Figure 5: The parameter $0.5\sqrt{\varepsilon}\beta_p \times \beta_t$ plotted vs. $1 + \kappa^2$. Each point represents the pulse average of one NSTX plasma discharge, with every discharge in the NSTX database plotted.

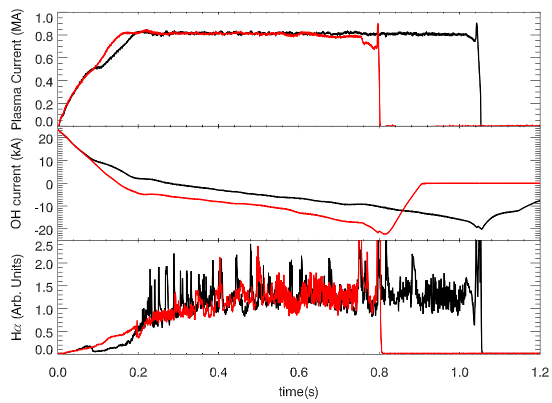

Figure 6: Figure showing the effect of the early H-mode transition on flux consumption a) Plasma current trace showing the programmed "flat-spot" in I_p which is used to trigger the transition b) the current in the Ohmic heating coil (proportional to the flux consumed) and c) the measured D_α emission showing the early H-mode (black, Shot 112546) occurs at the time of the "flat spot", whereas the normal H-mode transition (red, SHot 111964) is at the start of the I_p flat-top

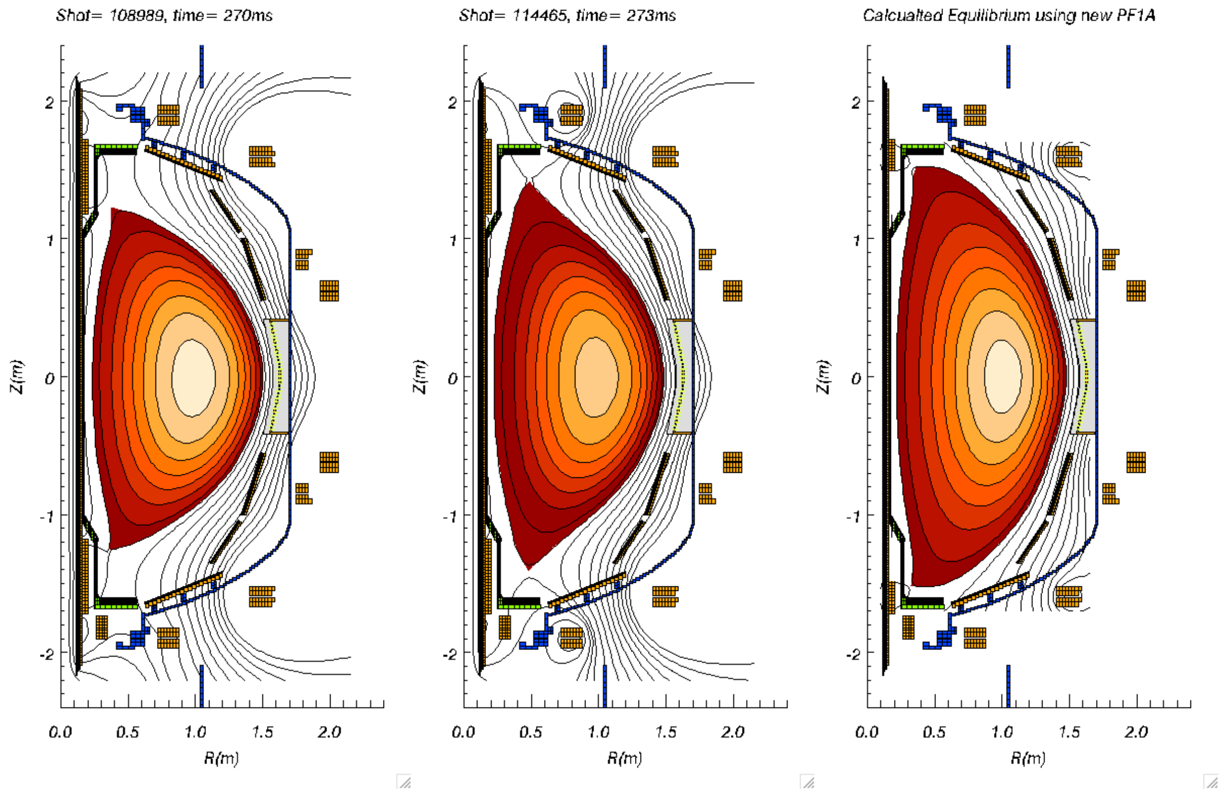

Figure 7: Evolution of the NSTX plasma shape from year to year a) high triangularity double null plasma from 2002 b) moderate triangularity high elongation double null from 2004, and c) a calculated high triangularity high elongation plasma which should be possible in 2005 as a result of the modification the PF1A coil

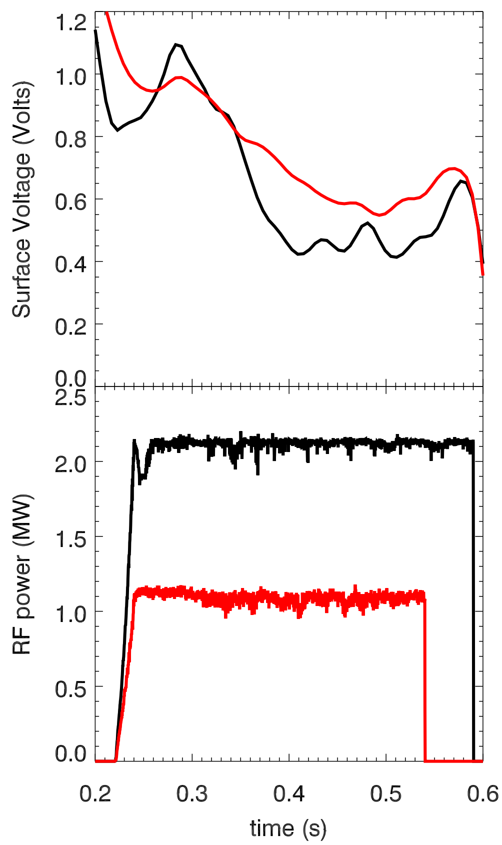

Figure 8: Results from an experiment deigned to demonstrate current drive using HHFW on NSTX. The first frame shows the measured loop voltage for two otherwise identical discharges for which the direction of the launched wavefront was reversed. The co-current phasing is Since the efficiency of heating varies substantially between co- and counter-phasing, the heating power (shown in the second frame) was adjusted until the mesured electron temperatures matched.

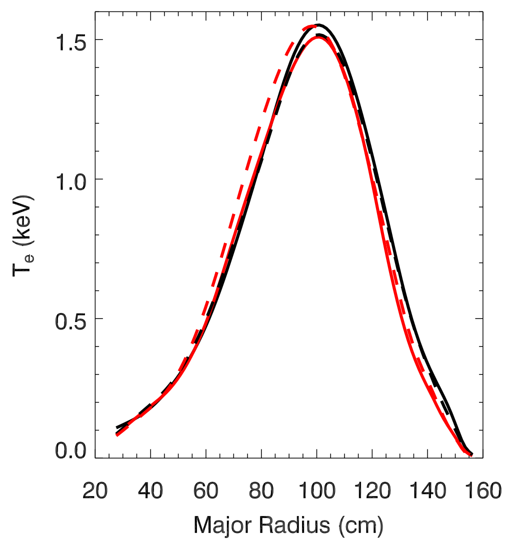

Figure 9: Comparison of the measured electron temperature profiles for 2 times for each discharge shown in Figure 8

External Distribution

Plasma Research Laboratory, Australian National University, Australia
Professor I.R. Jones, Flinders University, Australia
Professor João Canalle, Instituto de Fisica DEQ/IF - UERJ, Brazil
Mr. Gerson O. Ludwig, Instituto Nacional de Pesquisas, Brazil
Dr. P.H. Sakanaka, Instituto Fisica, Brazil
The Librarian, Culham Science Center, England
Mrs. S.A. Hutchinson, JET Library, England
Professor M.N. Bussac, Ecole Polytechnique, France
Librarian, Max-Planck-Institut für Plasmaphysik, Germany
Jolan Moldvai, Reports Library, Hungarian Academy of Sciences, Central Research Institute for Physics, Hungary
Dr. P. Kaw, Institute for Plasma Research, India
Ms. P.J. Pathak, Librarian, Institute for Plasma Research, India
Dr. Pandji Triadyaksa, Fakultas MIPA Universitas Diponegoro, Indonesia
Professor Sami Cuperman, Plasma Physics Group, Tel Aviv University, Israel
Ms. Clelia De Palo, Associazione EURATOM-ENEA, Italy
Dr. G. Grosso, Instituto di Fisica del Plasma, Italy
Librarian, Naka Fusion Research Establishment, JAERI, Japan
Library, Laboratory for Complex Energy Processes, Institute for Advanced Study, Kyoto University, Japan
Research Information Center, National Institute for Fusion Science, Japan
Dr. O. Mitarai, Kyushu Tokai University, Japan
Dr. Jiangang Li, Institute of Plasma Physics, Chinese Academy of Sciences, People's Republic of China
Professor Yuping Huo, School of Physical Science and Technology, People's Republic of China
Library, Academia Sinica, Institute of Plasma Physics, People's Republic of China
Librarian, Institute of Physics, Chinese Academy of Sciences, People's Republic of China
Dr. S. Mirnov, TRINITI, Troitsk, Russian Federation, Russia
Dr. V.S. Strelkov, Kurchatov Institute, Russian Federation, Russia
Professor Peter Lukac, Katedra Fyziky Plazmy MFF UK, Mlynska dolina F-2, Komenskeho Univerzita, SK-842 15 Bratislava, Slovakia
Dr. G.S. Lee, Korea Basic Science Institute, South Korea
Dr. Rasulkhozha S. Sharafiddinov, Theoretical Physics Division, Insitute of Nuclear Physics, Uzbekistan
Institute for Plasma Research, University of Maryland, USA
Librarian, Fusion Energy Division, Oak Ridge National Laboratory, USA
Librarian, Institute of Fusion Studies, University of Texas, USA
Librarian, Magnetic Fusion Program, Lawrence Livermore National Laboratory, USA
Library, General Atomics, USA
Plasma Physics Group, Fusion Energy Research Program, University of California at San Diego, USA
Plasma Physics Library, Columbia University, USA
Alkesh Punjabi, Center for Fusion Research and Training, Hampton University, USA
Dr. W.M. Stacey, Fusion Research Center, Georgia Institute of Technology, USA
Dr. John Willis, U.S. Department of Energy, Office of Fusion Energy Sciences, USA
Mr. Paul H. Wright, Indianapolis, Indiana, USA

03/07/05

The Princeton Plasma Physics Laboratory is operated
by Princeton University under contract
with the U.S. Department of Energy.

Information Services
Princeton Plasma Physics Laboratory
P.O. Box 451
Princeton, NJ 08543

Phone: 609-243-2750
Fax: 609-243-2751
e-mail: pppl_info@pppl.gov
Internet Address: http://www.pppl.gov